Neurol Sci (2013) 34:1917–1924
DOI 10.1007/s10072-013-1407-8

ORIGINAL ARTICLE

Age-related alteration in cerebral blood flow and energy failure is correlated with cognitive impairment in the senescence-accelerated prone mouse strain 8 (SAMP8)

Xuezhu Zhang · Guomin Li · Lin Guo · Kun Nie · Yujie Jia · Lan Zhao · Jianchun Yu

Received: 31 January 2013 / Accepted: 14 March 2013 / Published online: 7 April 2013

Abstract Cerebrovascular dysfunction is an early pathogenic event in Alzheimer's disease (AD) and plays a key role in the disease process. Cerebral hypoperfusion, brain glucose hypometabolism and disrupted blood–brain barrier (BBB) integrity contributed to the onset and progression of AD. However, the relationships between the age-related cognitive impairment and cerebral blood flow (CBF), energy metabolism and BBB have not been clearly explained. In this study, we investigated the cognitive function, CBF, BBB damage and expression level of glucose transporter (GLUT) 1 and 3 of senescence-accelerated mouse prone 8 (SAMP8), and the correlations between each of them were analyzed. When compared with SAMR1 (senescence-accelerated mouse resistant 1), the cognitive abilities of SAMP8 were damaged apparently even at 4 months of age, showing up a slower and more capricious acquisition in Morris water maze tasks. In both SAMP8 and SAMR1, reduced CBF and increased BBB leakage were observed with increasing age, but an earlier and more severe impairment was detected in SAMP8. In addition, alterations of GLUT1 and GLUT3 protein expression in cortex and hippocampus were more prominent in SAMP8. Correlation analysis demonstrated that the increased escape latency was correlated negatively with CBF and expression of glucose transporters; and positively with BBB permeability in the hippocampus. These results suggested that CBF, BBB integrity, the expression of GLUT1 and GLUT3 were significantly affected by age and strain, which were also closely associated with cognitive ability. The alteration in CBF and energy failure induced by aging and vascular insults resulted in cognitive decline in SAMP8.

Keywords Alzheimer's disease · Cerebral blood flow · Blood–brain barrier · Brain glucose metabolism

Xuezhu Zhang and Guomin Li have equally contributed to this work.

X. Zhang · G. Li · L. Guo · K. Nie · Y. Jia · L. Zhao · J. Yu (✉)
First Teaching Hospital of Tianjin University of Traditional Chinese Medicine, Tianjin 300193, China
e-mail: yujianchun2000@hotmail.com

X. Zhang
e-mail: zhangxuezhu1999@yahoo.com.cn

G. Li
First People's Hospital of Chenzhou City, Chenzhou 423000, Hunan Province, China

Introduction

Alzheimer's disease (AD) is a chronic degenerative disorder of the central nervous system characterized by insidious onset and progressive development. The loss of neuron, extracellular deposition of amyloid plaques and intracellular neurofibrillary tangles are the three primary pathological hallmarks of AD. Recent studies have found that vascular defect presented in AD is the key factor in the development of the disease [1]. Those data from clinical imaging, epidemiological and pharmacotherapy studies have proven that vascular changes have an essential role in early AD pathogenesis [2]. Magnetic resonance imaging (MRI) [3], transcranial Doppler measurements [4] and single-photon excitation computed tomography (SPECT) [5] in humans have confirmed that the cerebral blood flow (CBF) is significantly reduced in AD patients, suggesting an early event in AD pathogenesis, which is before the cognitive decline and brain atrophy [5]. With reduced CBF, the cerebral glucose metabolic rate in AD patients declined dramatically even before the emergence of cognitive

symptoms [6, 7], and significantly correlated with the severity of dementia [8]. The reduction in cerebral glucose metabolic rate was also observed before the onset of various diseases in several groups of at-risk individuals, including patients with mild cognitive impairment (MCI) [9], presymptomatic individuals carrying mutations responsible for early onset familial AD [7], cognitively normal elderly individuals who eventually declined to MCI and eventually to AD [6]; carriers of the apolipoprotein E epsilon-4 allele, a strong genetic risk factor for late-onset AD; and normal, middle-aged individuals, who expressed subjective memory complaints [10].

Therefore, abnormalities in CBF and energy metabolism of the brain could contribute to the onset and/or progression of neurodegenerative events in AD, and correlated positively with advanced age and dementia [11].

Senescence-accelerated mouse prone 8 (SAMP8) is a mouse strain characterized by an early onset of deficits in learning and memory. Cerebral atrophy, cortical and hippocampal neuron loss, β-amyloid deposition, hyperphosphorylation of tau, impaired development of dendritic spines, sponge formation and oxidative stress have also been detected in SAMP8 brain [12]. For these reasons, SAMP8 mice are regarded as an excellent model for studying AD. However, not much work has been done to determine the age-related deficits in cerebrovascular function, glucose uptake and energy metabolism and their correlations with cognitive impairment in SAMP8. To further clarify the underlying mechanism of cognitive dysfunction in SAMP8, the CBF, BBB integrity and the levels of major brain GLUTs were examined, and their effects on cognitive function of the mice were also discussed.

Materials and methods

Animals

Healthy male mice, obtained from our breeding colony, were assigned to one of the four groups ($n = 10$ per group) based on the strain (SAMR1/SAMP8) and age (4 months old/12 months old). The animals were housed in a pathogen-free, temperature and humidity-controlled environment providing a 12 h light–dark cycle, and allowed free access to purified water and a sterile diet containing 1.20 % calcium and 0.80 % phosphorus. All animals were maintained in accordance with Principles of laboratory animal care (NIH publication No. 86-23, revised 1985) and Guide for the Care and Use of Laboratory Animals, revised 2006 (Ministry of Science and Technology of the People's Republic of China), and animal protocols were approved by the Laboratory Animal Care Committee of the Tianjin University of Traditional Chinese Medicine.

Altogether, 80 SAM mice were included into this study and divided in two batches of 40 individuals each. The first batch of mice was used for evaluating the cognitive abilities and cerebral blood flow. The second batch was used for BBB function and western blot.

Morris water maze test

Morris water maze test was performed to evaluate the spatial reference memory of the mice. The water maze was a circular swim tank (90 cm in diameter and 50 cm in height) filled with water and temperature was maintained at 24 ± 1 °C. Non-toxic black latex paint was added to make the tank opaque. A transparent plastic escape platform with rough surface was submerged 1 cm below the water level. The water surface was divided into four quadrants (NE, SE, SW and NW) of equal size. Four starting positions were located in the middle of the four quadrants at the edge of the tank. Several distal visual cues were placed on the walls of the room. The swimming paths of the animals were recorded by a video camera mounted above the center of the tank. Before the trials, a new number (code) was assigned to each mouse by the same investigator (Xuezhu Zhang). Two other investigators (Jinfeng Liu and Lan Zhao), who were blinded to the grouping and codes, administrated the Morris water maze test.

During the hidden platform trial, each mouse performed eight trials per day for five consecutive days to locate the submerged platform. The platform was placed to the center in one of the tank quadrants during all the training days. On each trial, the mouse was placed gently into the water, facing the wall of the tank, in one of the four start locations. The order of the start locations was varied and any given sequence was not repeated on acquisition phase days. Each mouse was allowed to search for the platform for 60 s. Mouse was guide to hidden platform and remained on it for 10 s, if locating the platform was not able to complete within 60 s. The escape latency to locate the platform was measured in each trial. The mean escape latency of eight trials per day was calculated for each mouse.

A probe trial was conducted to evaluate the retention of each mouse in the location of the hidden platform. During the probe trial, the platform was removed from the pool and the animal was allowed to freely explore the pool for 60 s. The time spent in each quadrant, the number of crossing over the trained platform location and the distance swam was recorded.

Determination of cerebral blood flow

Mice were initially anaesthetized with isoflurane in 100 % O_2 (5 % induction, 2 % maintenance). Femoral artery was catheterized for continuous arterial pressure and heart rate

recording by a computerized data-acquisition system (PowerLab, ADInstruments) and for blood sampling. Animals were intubated and artificially ventilated with an O_2–N_2 mixture. The O_2 concentration in the mixture was adjusted to provide an arterial PO_2 of 120–150 mmHg. End-tidal CO_2, monitored by a CO_2 analyzer (Capstar-100, CWI), was controlled at 2.6–2.7 %. A heating lamp thermostatically controlled by a rectal probe was used to maintain the mouse body temperature at 37 ± 0.5 °C. After surgery, isoflurane was gradually discontinued, and anesthesia was continued with urethane (750 mg/kg, i.p.) and α-chloralose (50 mg/kg, i.p.). Anesthesia depth was assessed by testing the corneal reflexes and motor responses to the tail pinch. Throughout the experiment, two samples (50 μL) of arterial blood were collected for blood gas analysis.

Regional CBF was measured with a DRT4 laser Doppler blood flow and temperature monitor (Moor Instruments Inc). A midline skin incision, approximately 1 cm in length, was made parallel to the sagittal suture. The tip of the probe (Φ 2 mm) was stabilized to the intact skull 2 mm posterior to the bregma and 2 mm lateral to the sagittal suture using a tissue adhesive (Aron Alpha; Toa, Tokyo, Japan). After achieving a stable baseline, the CBF was continuously measured for 10 min. Zero value for CBF was determined by the end of the experiment, when the heart was stopped with an overdose of isoflurane.

Monitoring of blood–brain barrier permeability

Vascular permeability was quantitatively evaluated by fluorescent detection of extravasated Evans blue dye. In brief, 2 % Evans blue dye in saline was injected into the tail vain as a BBB permeability tracer. After 1 h, the Evans blue dye administration, the animals were deeply anesthetized with isoflurane and transcardially killed until colorless perfusion fluid was obtained from the right atrium. After decapitation, the cerebral cortex and hippocampus regions were isolated, weighted and homogenized in ninefold volume of 50 % trichloroacetic acid solution. The supernatant was obtained after centrifugation and diluted into threefold with ethanol. Samples and standards were loaded into a 96-well, flat-bottom, black-walled plate. Sample concentration was determined by a Varian Cary Eclipse Fluorescence Spectrophotometer (excitation 620 nm and emission 680 nm). The amount of extravasated Evans blue dye was quantified as micrograms per gram of brain tissue.

Western blot analysis of GLUTs expression

The tissues from cerebral cortex and hippocampus were homogenized in ice-cold RIPA buffer containing complete EDTA-free proteinase inhibitors (Roche). The homogenates were centrifuged at 12,000×g for 30 min, and the resulting supernatants were isolated for Western blot analyses after protein assay by BCA method. The samples were loaded on to 10 % SDS-PAGE, transferred to PVDF membrane, blocked with 5 % nonfat milk in TBS, and probed with rabbit anti-GLUT1 (1:2,000, Millipore), rabbit anti-GLUT3 (1:200, Abcam), or rabbit anti-β-actin (1:1,000, Santa Cruz) antibodies. Immunoreactive signals were detected with a Chemi Dos XRS system (Bio-Rad) after the reaction with Immobilon Western Chemiluminescent HRP Substrate (Millipore). Three mice from each group were chosen for preparation of the total protein extracts and each lysate sample was analyzed 3 times. The expression levels of target proteins were normalized to β-actin level in each sample, and the mean value of each group was calculated based on its own dataset.

Statistical methods

Mean and standard deviation (SD) were calculated for all results. The differences between groups were assessed by two-way ANOVA followed by LSD (equal variances assumed) or Dunnett's T3 (equal variances not assumed). For the Morris water maze tests, escape latency times in the hidden platform trial were analyzed with two-way ANOVA of repeated measures. The possible relationships between the cognitive impairment and other variables in mice were analyzed by Pearson's correlation coefficient. A significance level of $P < 0.05$ was used for all comparisons. All data analysis was performed using SPSS (version 13.0).

Results

Age-related cognitive impairment in mice

The SAMR1 mice at different ages all exhibited significantly improved performance during the hidden platform trial (Fig. 1), and they found their targets in much shorter time than the age-matched SAMP8. In contrast, the escape latencies of SAMP8 were not decreased significantly during the training period at both age groups. Except for the fourth day, in the same strain, no obvious age-related differences in escape latencies were found between the young and aged mice on any training day.

Marginal, random, tendency and linear searching strategies were searching strategies, employed by the animals to locate the platform. Almost all the mice failed to locate the platform on the first training day. Most of the animals swam around the tank wall and found the submerge platform by marginal or random searching strategy. Even though some mice successfully found the platform, they

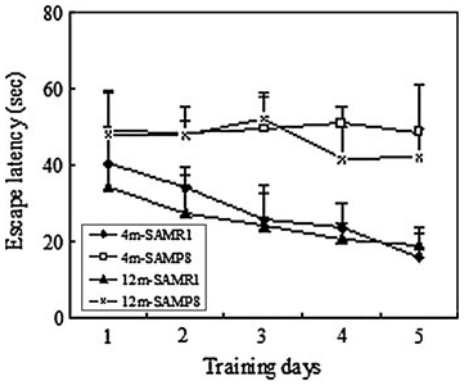

Fig. 1 Escape latency to find the hidden platform in Morris water maze test in mice. During the hidden platform trial, each mouse performed eight trials per day for five consecutive days to locate the submerged platform in a fixed location. The sequence of the start points was randomly varied on training phase. The escape latency (60 s maximum) was measured in each trial and the mean latency for each day was calculated for each mouse. Data are expressed as mean ± SE

were more likely to complete by chance. With the increase of training times, the SAMR1 gradually shifted their search patterns to the tendency or linear searching strategy, making their searching process more spatially precise and efficient. On the contrary, most of the SAMP8 were still in marginal or random searching pattern.

In the probe trail, there were significant strain-related differences between the SAMR1 and age-matched SAMP8, whereas the age differential was not a factor contributing to their performance. The SAMR1 at different ages spent significantly more time in the target quadrant than the SAMP8 ($P < 0.01$) (Fig. 2a). In addition, the number of crossings over the former platform location for SAMR1 was obviously larger ($P < 0.01$) (Fig. 2b). In addition, the distance swan for the SAMR1 was longer than that for the SAMP8 ($P < 0.01$) (Fig. 2c). No significant age-dependent differences in behavioral performance were identified between the any two groups of the same strain. The results of the probe trial suggested a certain degree of spatial learning deficit in the SAMP8.

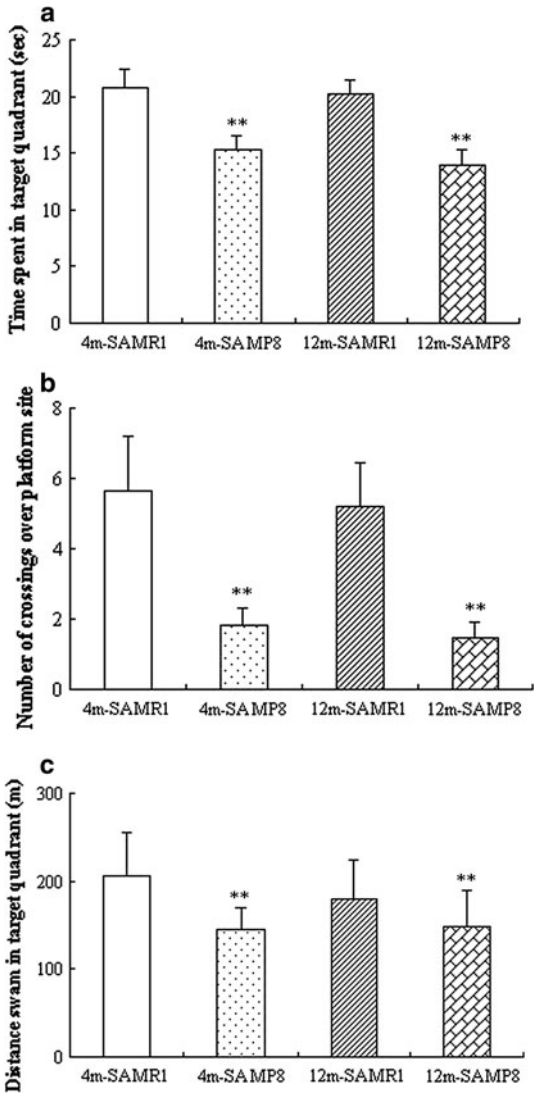

Fig. 2 The probe trial performance of the SAMR1 and SAMP8 mice. During the probe trial, the platform was removed from the pool and the animal was allowed to swim freely in the pool for 60 s. **a** The time spent in the target quadrant during the probe trial. **b** The number of crossings over the platform position in the target quadrant during the probe trial. **c** Total distance swam in the target quadrant during the probe trial. When compared with the age-matched SAMR1, $^{**}P < 0.01$

Regional CBF in mice

Notable strain-associated differences were observed in CBF between the SAMR1 and SAMP8 at the same age (Fig. 3). The CBF obviously declined 15.07 and 17.80 % for 4- and 12-month-old SAMP8 than the age-matched SAMR1, respectively ($P < 0.05$, $P < 0.01$). The CBF of aged SAMP8 decreased sharply by nearly 11 % than the young mice ($P < 0.05$). As to the SAMR1, the reduced CBF was detected in the aged mice, but the difference did not reach the statistical significance level.

Blood–brain barrier integrity in mice

In the cerebral cortex, no prominent age-associated and strain-specific differences were detected in BBB permeability between any two groups. However, in the hippocampus, the BBB integrity was altered obviously with the age and strain. Within the same strain, the aged mice showed significantly increased BBB leakage than the young mice (Fig. 4). When compared with the young mice of the same strain, the Evans blue content in hippocampus of aged SAMR1 and SAMP8 elevated 47.49 and 67.18 %,

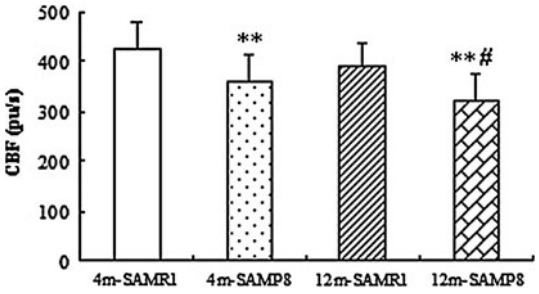

Fig. 3 Regional cerebral blood flow in SAMR1 and SAMP8 mice. The mice were anaesthetized and the femoral artery was catheterized for continuous arterial pressure, heart rate, end-tidal CO_2 and blood gas measurement. Then, a midline incision was made and the skull was exposed. A laser-Doppler probe was fixed onto the intact skull and the regional CBF was continuously recorded for 10 min after baseline was stable. When compared with the age-matched SAMR1, $^{*}P < 0.05$; $^{**}P < 0.01$; when compared with the young mice of the same strain, $^{\#}P < 0.05$

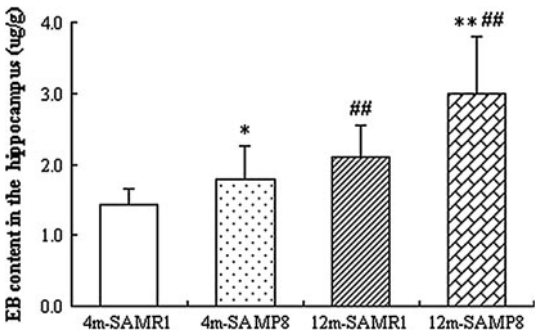

Fig. 4 Blood–brain barrier integrity in the hippocampus of SAMR1 and SAMP8 mice. The Evans blue dye (2 % in saline) was injected into the tail vain of the mice. One hour later, the mice were anesthetized and perfused with saline to wash out any remaining dye in the blood vessels. The brains were removed and the cortical and hippocampal tissues were isolated, weighted, homogenized in 50 % trichloroacetic acid solution and centrifuged. Then the supernatant was diluted by ethanol and analyzed by a fluorescence spectrophotometer with excitation at 620 nm and emission at 680 nm. The concentration of the dye was calculated using a standard curve. When compared with the age-matched SAMR1, $^{*}P < 0.05$; $^{**}P < 0.01$; when compared with the young mice of the same strain, $^{\#\#}P < 0.01$

respectively ($P < 0.01$). In addition, BBB permeability was notably increased in SAMP8 when compared with age-matched SAMR1. The dye content of hippocampus significantly elevated 25.82 and 42.61 % for 4- and 12-month-old SAMP8 than the age-matched SAMR1, respectively ($P < 0.05$, $P < 0.01$).

Expression of the GLUTs in brain

GLUT1 and GLUT3 expression were found significantly different in age and strain (Fig. 5). When compared with the age-matched SAMR1, obviously elevated GLUT1 was detected in both the cortex and hippocampus of 4-months-old SAMP8 ($P < 0.05$), while the expression of GLUT3 was significantly increased in the cortex but decreased in the hippocampus ($P < 0.05$). Besides increased GLUT1 protein level in the cortex, both GLUT1 and GLUT3 expression in 12-month-old SAMP8 declined in comparison with the age-matched SAMR1 ($P < 0.05$). Furthermore, as compared to the young mice of the same strain, significantly increased GLUT1 and decreased GLUT3 expression were detected in both the cortex and

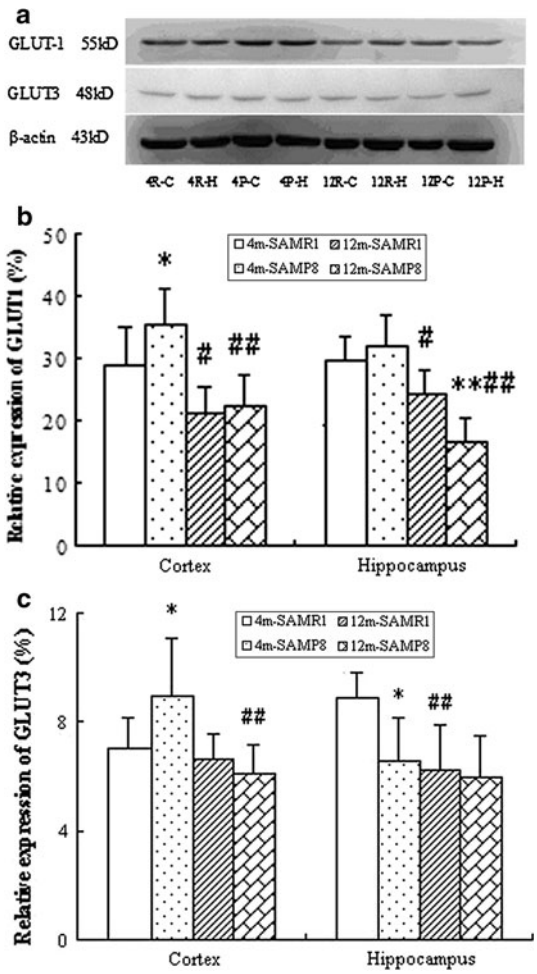

Fig. 5 Western blot analysis of GLUT1 and GLUT3 proteins in the cortex and hippocampus of mice. The cortex and hippocampus lysates of mice were resolved by electrophoresis, transferred to PVDF membrane, and probed with antibodies specific to the target proteins. The expression levels of target proteins were normalized to β-actin level in each sample. **a** Representative western blot image from the SAMR1 and SAMP8 mice. From *left* to *right*, the image showed cortex in 4 m-SAMR1, hippocampus in 4 m-SAMR1, cortex in 4 m-SAMP8, hippocampus in 4 m-SAMP8, cortex in 12 m-SAMR1, hippocampus in 12 m-SAMR1, cortex in 12 m-SAMP8 and hippocampus in 12 m-SAMP8. **b** The relative expression levels of GLUT1 protein in cortex and hippocampus of mice. **c** The relative expression levels of GLUT3 protein in cortex and hippocampus of mice. When compared with the age-matched SAMR1, $^{*}P < 0.05$, $^{**}P < 0.01$; as compared to the young mice of the same strain, $^{\#}P < 0.05$, $^{\#\#}P < 0.01$

Table 1 Correlations between the cognitive impairment and other variables

Variables	4 m-SAMR1	4 m-SAMP8	12 m-SAMR1	12 m-SAMP8
CBF	−0.076	−0.513**	−0.203	−0.632**
BBB permeability in cortex	0.068	0.252	0.116	0.360*
BBB permeability in hippocampus	0.136	0.442**	0.313*	0.625**
GLUT-1 expression in cortex	−0.055	−0.274*	−0.154	−0.318*
GLUT-1 expression in hippocampus	−0.086	−0.348*	−0.280	−0.427**
GLUT-3 expression in cortex	−0.102	−0.253*	−0.309*	−0.362**
GLUT-3 expression in hippocampus	−0.094	−0.397**	−0.332*	−0.445**

*$P < 0.05$; **$P < 0.01$

hippocampus of aged SAMR1 ($P < 0.05$). However, the expression of GLUT1 in the hippocampus and GLUT3 in the cortex of aged SAMP8 declined obviously than the young mice ($P < 0.05$).

Correlations between cognitive function and related factors in mice

The relationships between the impairment of spatial cognitive performance (escape latency) and regional CBF, BBB permeability, the expression of GLUT1 and GLUT3 of the mice were analyzed by Pearson's correlation coefficient (Table 1). As displayed in Table 1, cognitive impairment was correlated negatively with regional CBF ($P < 0.01$); and positively with BBB permeability in hippocampus ($P < 0.01$). There were significant negative correlations between the cognitive function and GLUT1 and GLUT3 expression in the cortex and hippocampus ($P < 0.01$).

Discussion

Alzheimer's disease (AD) is an age-related neurodegenerative disease characterized by a progressive loss of cognitive and functional abilities associated with various behavioral disturbances. In recent years, an increasing attention has been paid on the cerebrovascular defects and BBB impairment, which are presented and occurred early in AD. However, the roles of vascular dysfunction in the pathogenesis of the disease and related molecular mechanisms are not fully understand, and appropriate animal models are unavailable, which all limit the development of more effective diagnostic and therapeutic strategies for AD.

The brain is metabolically active and demands a large and continual supply of energy. However, the brain has very small energy reserves, which makes the maintenance of brain function depending entirely on an adequate supply of vascular perfusion, glucose and oxygen. Cerebral vascular injury, reduced cerebral blood flow, and/or decreased glucose metabolism all can lead to neural damage or death, even declines in cognitive abilities.

Several studies have demonstrated a significantly decreased rCBF in MCI and AD patients [3, 5]. Low CBF may be an early contributor to the progression of dementia, prior to the cognitive decline and cerebral atrophy [4]. In this study, both age- and strain-related decreases in CBF were clearly detected in SAMR1 and SAMP8 mice, but the magnitude of these changes was more pronounced in SAMP8. Furthermore, the declined CBF and its close correlation with cognitive deficits suggested that the alterations in CBF may contribute to the cerebral pathology observed in SAMP8.

Clinical topographical imaging has shown that cerebral microbleedings were present in roughly 30 % of AD cases [13]. AD was more severe in the presence of established cerebral infarction [14], and autopsy studies showed 70 % of the AD patients to have evidence of coexistent cerebrovascular disease and 35 % to have had a cerebral infarction [15]. Even if a significant cerebrovascular disease was removed and vascular risk factors were minimized by exclusion of elevated Hachinski ischemia scores, 22 % of the mild to moderate AD patients still exhibited BBB impairment. The degree of BBB lesions was correlated with the rates of disease progression, including annual change in MMSE and Annual Clinical Dementia Rating sum-of-boxes change [16]. In this study, both age-related and strain-associated BBB impairments were detected in hippocampus of SAMR1 and SAMP8 mice, and the lesion was more obvious in SAMP8 than in SAMR1. Our results corroborated the findings of previous works, in which either exogenous dyes [17] or endogenous IgG [18] was used as tracers to evaluate BBB function. The increased BBB permeability with age and its strong relationship with cognitive deficits suggested that BBB impairment in SAMP8 involved in hippocampal dysfunctions, such as age-related cognitive deficits and neuronal death.

In addition to decreased CBF, the cerebral glucose transport across the BBB and the phosphorylation rates measured by FDG-PET were reduced in hypometabolic regions in MCI and AD patients [19–24]. The reduction was more pronounced in hippocampus and posterior cingulated cortex in mild dementia, and gradually extends to parieto-temporal regions in moderate-to-severe AD [20, 21, 23, 25]. GLUT1 and GLUT3 are the main glucose transporters in the brain. GLUT1 (55kD) is primarily expressed in the capillary endothelial cells of the BBB, whereas

GLUT3 is enriched in neurons. They are responsible for glucose transport across the BBB and into neurons, and their expression levels are regulated by blood glucose concentration and hypoxia–ischemia in the brain [26, 27]. In this study, alterations in GLUT1 and GLUT3 expression levels were identified in the cortex and hippocampus of SAMP8 and SAMR1 at different ages. 4 months of age may be the early stage of cognitive impairments in SAMP8. At this time point, declined glucose supply due to reduced CBF in cortex could be compensated by enhancing GLUTs expression and promoting glucose transmembrane transport. However, parallel changes were not observed in hippocampus. The increased GLUT1 and decreased GLUT3 in hippocampus of 4-month-old SAMP8 suggested that the glucose, entered into brain interstitial fluid from BBB, was not transported efficiently into hippocampal neurons to eliminate their energy deficits. Because hippocampal neurons are vulnerable to hypoxic/ischemic injury [28], insufficient energy supply leads to neuronal damage and loss which caused a further decline in brain energy demand as well as glucose transporters expression [29]. Therefore, the decreased GLUT3 expression in hippocampus of SAMP8 might be the result of neuron dysfunction. At 12 months of age, accompanied by the more severe cerebral ischemia, the expression levels of GLUT1 and GLUT3 protein were decreased in both the cortical and hippocampal tissues when compared with the 4-month age-matched controls. These data suggested that the cortical neurons were damaged significantly and their energy demand was reduced at the age of 12 months; while energy failure in hippocampus still persisted.

During the entire study period, SAMP8 mice at different ages exhibited impaired learning and memory abilities. The cognitive decline in SAMP8 was detected obviously even at 4 months of age, which has not been described previously. No significant age-related differences in cognitive abilities were found in the mice of the same strain, suggesting that strain, but not age, is a more important factor affecting cognitive performance of the mice. As one part of the limbic system, hippocampus is important for short-term memory and spatial navigation. In this study, distorted regional CBF, BBB integrity and impaired glucose uptake in hippocampus, and their strong association with cognitive function provided direct indexes of neuron loss in SAMP8.

Torre [30] proposed the CATCH hypothesis (critically attained threshold of cerebral hypoperfusion) to explain the pathogenesis of AD. According to the hypothesis, advanced aging together with vascular risk factors predisposing to cerebral hypoperfusion created CATCH in brain. CATCH induces brain capillary degeneration and suboptimal delivery of energy substrates to neuronal tissue. The outcome of this defect generated a chain of events leading to the progressive evolution of brain metabolic, cognitive and tissue pathology that characterize Alzheimer's disease. The results of our study confirmed the viewpoint.

Taken together, the distorted regional brain microcirculation and impaired optimal delivery of energy substrates caused by aging and ischemia were the crucial players in the initiation and progression of cognitive decline of SAMP8. The SAMP8 mice appear to be an excellent rodent model to study the cerebrovascular dysfunction and glucose hypometabolism seen in Alzheimer disease.

References

1. Scheibel AB, Duong TH, Jacobs R (1989) Alzheimer's disease as a capillary dementia. Ann Med 21:103–107
2. de la Torre JC (2004) Is Alzheimer's disease a neurodegenerative or a vascular disorder? data, dogma, and dialectics. Lancet Neurol 3:184–190
3. Johnson NA, Jahng GH, Weiner MW, Miller BL, Chui HC, Jagust WJ, Gorno-Tempini ML, Schuff N (2005) Pattern of cerebral hypoperfusion in Alzheimer disease and mild cognitive impairment measured with arterial spin-labeling MR imaging: initial experience. Radiology 234:851–859
4. Ruitenberg A, den Heijer T, Bakker SL, van Swieten JC, Koudstaal PJ, Hofman A, Breteler MM (2005) Cerebral hypoperfusion and clinical onset of dementia: the rotterdam study. Ann Neurol 57(6):789–794
5. Hirao K, Ohnishi T, Hirata Y, Yamashita F, Mori T, Moriguchi Y, Matsuda H, Nemoto K, Imabayashi E, Yamada M, Iwamoto T, Arima K, Asada T (2005) The prediction of rapid conversion to Alzheimer's disease in mild cognitive impairment using regional cerebral blood flow SPECT. Neuroimage 28:1014–1021
6. Mosconi L, De Santi S, Li J, Tsui WH, Li Y, Boppana M, Laska E, Rusinek H, de Leon MJ (2008) Hippocampal hypometabolism predicts cognitive decline from normal aging. Neurobiol Aging 29(5):676–692
7. Mosconi L, Sorbi S, de Leon MJ, Li Y, Nacmias B, Myoung PS, Tsui W, Ginestroni A, Bessi V, Fayyazz M, Caffarra P, Pupi A (2006) Hypometabolism exceeds atrophy in presymptomatic early-onset familial Alzheimer's disease. J Nucl Med 47(11): 1778–1786
8. Blass JP (2002) Alzheimer's disease and Alzheimer's dementia: distinct but overlapping entities. Neurobiol Aging 23(6): 1077–1084
9. Mosconi L, Tsui WH, De Santi S, Li J, Rusinek H, Convit A, Li Y, Boppana M, de Leon MJ (2005) Reduced hippocampal metabolism in MCI and AD: automated FDG-PET image analysis. Neurology 64(11):1860–1867
10. Mosconi L, De Santi S, Brys M, Tsui WH, Pirraglia E, Glodzik-Sobanska L, Rich KE, Switalski R, Mehta PD, Pratico D, Zinkowski R, Blennow K, de Leon MJ (2008) Hypometabolism and altered cerebrospinal fluid markers in normal apolipoprotein E E4 carriers with subjective memory complaints. Biol Psychiatry 63(6):609–618
11. Desgranges B, Baron JC, de la Sayette V, Petit-Taboué MC, Benali K, Landeau B, Lechevalier B, Eustache F (1998) The neural substrates of memory systems impairment in Alzheimer's disease: a PET study of resting brain glucose utilization. Brain 121(Pt4):611–631
12. Morley JE, Kumar VB, Bernardo AE, Farr SA, Uezu K, Tumosa N, Flood JF (2000) Beta-amyloid precursor polypeptide in SAMP8 mice affects learning and memory. Peptides 21(12): 1761–1767

13. Pettersen JA, Sathiyamoorthy G, Gao FQ, Szilagyi G, Nadkarni NK, St George-Hyslop P, Rogaeva E, Black SE (2008) Microbleed topography, leukoaraiosis, and cognition in probable Alzheimer disease from the sunnybrook dementia study. Arch Neurol 65:790–795
14. Heyman A, Fillenbaum GG, Welsh-Bohmer KA, Gearing M, Mirra SS, Mohs RC, Peterson BL, Pieper CF (1998) Cerebral infarcts in patients with autopsy-proven Alzheimer's disease: CERAD, part XVIII. Consortium to establish a registry for Alzheimer's disease. Neurology 51(1):159–162
15. Kalaria RN (2003) Vascular factors in Alzheimer's disease. Int Psychogeriatr 15(Suppl 1):47–52
16. Bowman GL, Kaye JA, Moore M, Waichunas D, Carlson NE, Quinn JF (2007) Blood–brain barrier impairment in Alzheimer disease: stability and functional significance. Neurology 68(21): 1809–1814
17. Del Valle J, Duran-Vilaregut J, Manich G, Camins A, Pallàs M, Vilaplana J, Pelegrí C (2009) Time-course of blood–brain barrier disruption in senescence-accelerated mouse prone 8 (SAMP8) mice. Int J Dev Neurosci 27(1):47–52
18. Pelegrí C, Canudas AM, del Valle J, Casadesus G, Smith MA, Camins A, Pallàs M, Vilaplana J (2007) Increased permeability of blood–brain barrier on the hippocampus of a murine model of senescence. Mech Ageing Dev 128(9):522–528
19. Drzezga A, Lautenschlager N, Siebner H, Riemenschneider M, Willoch F, Minoshima S, Schwaiger M, Kurz A (2003) Cerebral metabolic changes accompanying conversion of mild cognitive impairment into Alzheimer's disease: a PET follow-up study. Eur J Nucl Med Mol Imaging 30:1104–1113
20. Friedland RP, Jagust WJ, Huesman RH, Koss E, Knittel B, Mathis CA, Ober BA, Mazoyer BM, Budinger TF (1989) Regional cerebral glucose transport and utilization in Alzheimer's disease. Neurology 39(11):1427–1434
21. Jagust WJ, Seab JP, Huesman RH, Valk PE, Mathis CA, Reed BR, Coxson PG, Budinger TF (1991) Diminished glucose transport in Alzheimer's disease: dynamic PET studies. J Cereb Blood Flow Metab 11(2):323–330
22. Hunt A, Schonknecht P, Henze M, Seidl U, Haberkorn U, Schroder J (2007) Reduced cerebral glucose metabolism in patients at risk for Alzheimer's disease. Psychiatry Res 155:147–154
23. Piert M, Koeppe RA, Giordani B, Berent S, Kuhl DE (1996) Diminished glucose transport and phosphorylation in Alzheimer's disease determined by dynamic FDG-PET. J Nucl Med 37(2):201–208
24. Shim YS, Morris JC (2011) Biomarkers predicting Alzheimer's disease in cognitively normal aging. J Clin Neurol 7(2):60–68
25. Mosconi L, Tsui WH, Rusinek H, De Santi S, Li Y, Wang GJ, Pupi A, Fowler J, de Leon MJ (2007) Quantitation, regional vulnerability and kinetic modeling of brain glucose metabolism in mild Alzheimer's disease. Eur J Nucl Med Mol Imaging 34:1467–1479
26. Tanaka T, Wakamatsu T, Daijo H, Oda S, Kai S, Adachi T, Kizaka-Kondoh S, Fukuda K, Hirota K (2010) Persisting mild hypothermia suppresses hypoxia-inducible factor-1alpha protein synthesis and hypoxia-inducible factor-1-mediated gene expression. Am J Physiol Regul Integr Comp Physiol 298(3):R661–R671
27. Zovein A, Flowers-Ziegler J, Thamotharan S, Shin D, Sankar R, Nguyen K, Gambhir S, Devaskar SU (2004) Postnatal hypoxic-ischemic brain injury alters mechanisms mediating neuronal glucose transport. Am J Physiol Regul Integr Comp Physiol 286(2):R273–R282
28. O'Sullivan M (2008) Leukoaraiosis. Pract Neurol 8(1):26–38
29. Pietrini P, Furey ML, Alexander GE, Mentis MJ, Dani A, Guazzelli M, Rapoport SI, Schapiro MB (1999) Association between brain functional failure and dementia severity in Alzheimer's disease: resting versus stimulation PET study. Am J Psychiatry 156(3):470–473
30. de la Torre JC (2008) Pathophysiology of neuronal energy crisis in Alzheimer's disease. Neurodegener Dis 5(3–4):126–132